Processes triggered in guanine quadruplexes by direct absorption of UV radiation: From fundamental studies toward optoelectronic biosensors

Dimitra Markovitsi

Received: 3 May 2023 | Revised: 29 May 2023 | Accepted: 30 May 2023

DOI: 10.1111/php.13826

INVITED REVIEW

Processes triggered in guanine quadruplexes by direct absorption of UV radiation: From fundamental studies toward optoelectronic biosensors

Dimitra Markovitsi

CNRS, Institut de Chimie Physique, UMR8000, Université Paris-Saclay, Orsay, France

Correspondence
Dimitra Markovitsi, CNRS, Institut de Chimie Physique, UMR8000, Université Paris-Saclay, 91405 Orsay, France.
Email: dimitra.markovitsi@universite-paris-saclay.fr

Abstract

Guanine quadruplexes (GQs) are four-stranded DNA/RNA structures exhibiting an important polymorphism. During the past two decades, their study by time-resolved spectroscopy, from femtoseconds to milliseconds, associated to computational methods, shed light on the primary processes occurring when they absorb UV radiation. Quite recently, their utilization in label-free and dye-free biosensors was explored by a few groups. In view of such developments, this review discusses the outcomes of the fundamental studies that could contribute to the design of future optoelectronic biosensors using fluorescence or charge carriers stemming directly from GQs, without mediation of other molecules, as it is the currently the case. It explains how the excited state relaxation influences both the fluorescence intensity and the efficiency of low-energy photoionization, occurring via a complex mechanism. The corresponding quantum yields, determined with excitation at 266/267 nm, fall in the range of $(3.0–9.5)\times10^{-4}$ and $(3.2–9.2)\times10^{-3}$, respectively. These values, significantly higher than the corresponding values found for duplexes, depend strongly on certain structural factors (molecularity, metal cations, peripheral bases, number of tetrads ...) which intervene in the relaxation process. Accordingly, these features can be tuned to optimize the desired signal.

KEYWORDS

bionsensors, charge carriers, excited state relaxation, G-Quadruplexes, intrinsic fluorescence, optoelectronics, photoionization, time-resolved spectroscopy

Abbreviations: dGMP, 2′-deoxyguanosine 5′-monophosphate; fs-TA, femtosecond transient absorption; fs-TRF, femtosecond time-resolved fluorescence; FU, fluorescence upconversion; G-wires, guanine wires; ns-TA, nanosecond transient absorption; OXY, base sequence containing the *oxytricha nova* telomeric repeat TTTTGGGG; TEL, base sequence containing the human telomeric repeat TTAGGG; TSCPC, time-correlated single photon counting; 1-M, monomolecular; 2-M, bimolecular; 4-M, tetramolecular.

This article is part of a Special Issue dedicated to the topic of Nucleic Acid Photophysics.

INTRODUCTION

Guanine quadruplexes (GQs) are DNA/RNA structures formed by guanine rich strands of nucleic acids. Their building blocks are guanine tetrads in which each guanine is connected to two others via hydrogen bonds involving four different positions (Figure 1A). They may result from the folding of one strand or the association of two three or four strands and are called, respectively, monomolecular, bimolecular, or tetramolecular GQs. Helically stacked tetrads constitute the guanine core; monovalent cations, such as K^+ or Na^+, located in the central cavity of the core, contribute to the stability of the structure. Besides the guanines of the core, GQs contain also peripheral nucleobases which are located in loops connecting the tetrads and/or at capping groups at the end the strands (Figure 2B). In addition to these structural features, which will be discussed herein, GQs exhibit a rich polymorphism, including formation of higher order structures.[1]

Guanine quadruplexes play an important role in key biological functions (gene expression, replication, transcription, genome stability, epigenetic regulation ...). They are being correlated, in a positive or negative way, with an increasing number of pathologies, from cancer to neurodegenerative disorders[2–4] and viral infections, including COVID-19.[5,6] This knowledge has prompted therapeutic strategies targeting GQs with the aim to either stabilize or destabilize them.[7–9]

Beyond therapeutics, an intense activity is dedicated to the development of devices utilizing the unique properties of GQs for various applications in the field of nanoelectronics.[10] GQ-based biosensors[11–14] detect biomarkers typical of precise pathologies, as for example, abnormal concentration of K^+ in the blood of patients undergoing hemodialysis,[15] the presence of SARS-CoV-2[16] or that of short DNA fragments (cfDNA) in the plasma of patients with cancer.[17] Sensors operating on similar principles are also used for the detection of chemicals detrimental to the health, such carcinogenic azo dyes encountered as food additives,[18] or Pb^{2+} ions in aquatic products.[19] Most commonly, detection is achieved through optical and/or electrochemical methods and requires the mediation of an appropriate label chemically attached to the nucleic acid, or of a dye simply interacting with the GQ structure (label-free sensors).

But it is well established by now that optical signals (fluorescence emission), as well as charge carriers can be generated upon direct excitation of DNA. And most importantly, the signals stemming from GQs are more intense compared to those originating from other DNA structures.[20,21] The demonstration that self-association of guanine-rich DNA strands can be probed by following their intrinsic fluorescence dates back to 2004[22] (Figure 2), while that of UV-induced charge carrier generation was published just on 2017.[23] Interestingly, the GQ photoionization was observed at low energy (4.7 eV/266 nm), where the aqueous solvent is not reactive. This is an important advantage for applications, because the origin of the generated signals can be clearly correlated with the GQs.

Since the two premieres mentioned above, numerous studies, both experimental and computational, have been dedicated to the characterization of the primary processes underlying fluorescence emission and generation of charge carriers in DNA GQs triggered by direct absorption of UV radiation. To this end, UV-induced changes in optical signals were explored from the femtosecond to the millisecond timescales, in parallel with other DNA structures, and their interpretation was rationalized by quantum chemistry calculations. These results were

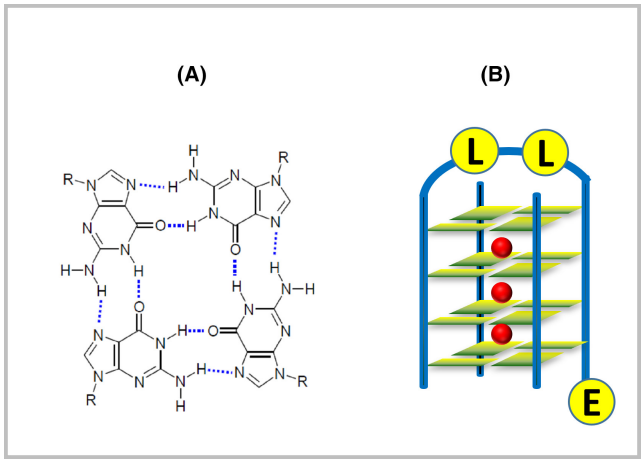

FIGURE 1 Schematic representation of a guanine tetrad (A) and a GQ formed by association of three strands (B); red spheres in (B) correspond to metal cations (K^+, Na^+); L and E indicate the peripheral nucleobases located, respectively, at the loop and the capping group.

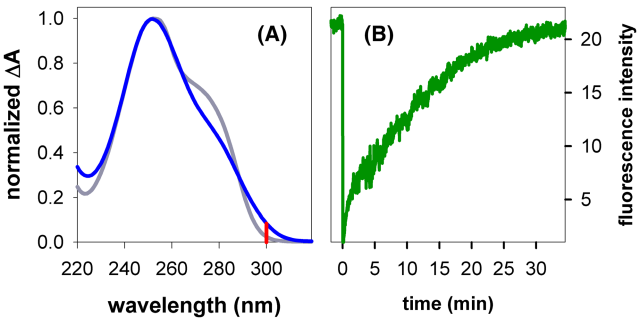

FIGURE 2 (A) Normalized absorption spectra of $(G_3)_4/Na^+$ (blue) and deoxyguanosine monophosphate (dGMP, gray) at room temperature; the vertical line indicates the excitation wavelength used to monitor the fluorescence of a $(G_3)_4/Na^+$ solution at 380 nm (B); at zero-time, the solution was heated at 80°C and then left to be cooled slowly at room temperature.[22]

highlighted in references Balanikas et al., Gustavsson and Markovitsi, Balanikas and Markovitsi, and Martinez-Fernandez et al.,[20,21,24,25] dealing with nucleic acids in general, and providing detailed description of the various methodologies and concepts used in these studies.

Quite recently, the use of the intrinsic DNA fluorescence, and in particular that of the GQs, for analytical purposes started to be explored. The motivation for the development of such label-free and dye-free devices is that they circumvent the synthesis of nucleic acids with appropriate labels or the caveats arising from non-covalent interactions between the nucleic acids and the dyes playing the role of mediators. Guo and coworkers constructed an easy to manipulate DNA detection system exploiting the fluorescence of an interlocked bimolecular GQ.[26] Zuffo et al.,[27] tested, by means of multivariate analysis, the applicability of the DNA fluorescence in assays aiming at the screening a large number of sequences. Liu et al. examined the possibility to probe target molecules (caffeine, cortisol ...) and metal ions (Pb^{2+}, Mg^{+2}, Sr^{2+} ...) by observing the intrinsic GQ fluorescence.[28,29] Finally, synchronous fluorescence spectroscopy and multivariate data analysis was proposed for the authentication of Covid-19 vaccines.[30]

Within this context, the present review describes the main outcomes of the fundamental studies on the processes triggered in GQs by direct absorption of UV radiation. It discusses the reasons for which certain structural parameters (molecularity, topology, peripheral bases, and metal cations in the central cavity) affect, on the one hand, the fluorescence quantum yield Φ_{fl} and the fluorescence spectral shape, and on the other, the photoionization quantum yield Φ_i. Although similar questions have been addressed in phenomenological studies carried out by steady-state measurements,[31–35] the knowledge of the underlying primary processes offers a different perspective.

Below, we first introduce the GQ structures studied by various time-resolved techniques. In the subsequent section, we provide a brief description of the main electronic and structural modifications occurring upon the absorption of a single UV photon by a GQ. The pathways followed during the excited state relaxation are crucial for both fluorescence emission and charge carrier generation, which are discussed in the next two sections. Finally, we highlight the structural factors that can be controlled to maximize the UV-induced "intrinsic GQ signals" in view of their application in optoelectronic biosensors and suggest some further investigations.

SYSTEMS AND TECHNIQUES

The GQs investigated by time-resolved spectroscopic techniques are listed in Table 1; according to the type of metal cation M^+ used (Na^+ or K^+), they are noted as "abbreviation/M^+". Their peripheral nucleobases are thymines and/or adenines. In most of the experiments, GQs were dissolved in phosphate buffer, and, alternatively, in KCl or NaCl. The purity of the oligonucleotides, as well as that of the salts and the water used in the preparation of the solutions are of paramount importance. Impurities may interact with GQs and give rise to red-shifted fluorescence, behaving, in a certain way, as the biosensor mediators.

TABLE 1 DNA GQs studied by time-resolved spectroscopy.

Type[a]	Sequence (5′–3′)	Abbreviation	Techniques
1-M	$G_{(\sim 3600)}$	G-wires	TCSPC[38–40]
	$TAG_3(T_2AG_3)_3T_2$	TEL25[b]	ns-TA[55]
	$G_3(T_2AG_3)_3$	TEL21[b]	FU/TCSPC[45,60]; fs-TRF/fs-TA[37]; ns TA[23,71]
2-M	$G_4T_4G_4$	OXY[c]	FU/TCSPC,[36] ns-TA[20]
4-M	TG_5T	$(TG_5T)_4$	FU/TCSPC[64]
	TG_4T	$(TG_4T)_4$	FU/TCSPC[40,65]; ns-TA[70,72,92]
	TG_3T	$(TG_3T)_4$	FU/TCSPC[64]
	TG_4	$(TG_4)_4$	ns-TA[48]
	G_4T	$(G_4T)_4$	ns-TA[48]
	AG_5A	$(AG_4A)_4$	ns-TA[48]
	AG_5	$(AG_4)_4$	ns-TA[48]
	G_4A	$(G_4A)_4$/	ns-TA[48]
	TAG_4AT	$(TAG_4AT)_4$	ns-TA[48]
	G_3	$(G_3)_4$	FU[22]

[a]Monomolecular (1-M), bimolecular (2-M), and tetramolecular (4-M).

[b]TEL: containing the human telomeric repeat TTAGGG.

[c]OXY: containing the *Oxytricha nova* telomeric repeat TTTTGGGG.

Moreover, they may also chemically react with the guanine radicals, altering their reaction path. The protocols followed in our group can be found, for example, in reference Balanikas et al.[20] and the Supporting Information of reference Balanikas et al.[36]

We studied fluorescence from the fs to the ns timescales using as excitation source fs laser pulses and two different detection techniques, fluorescence upconversion (FU) and time-correlated single photon counting (TCSPC). The generation and the reaction dynamics of charge carriers were probed from the ns to the ms timescales by ns transient absorption spectroscopy (ns-TA), using as excitation source 5 ns laser pulses. The latter technique allows detecting transient species in very low concentrations, which cannot be achieved by fs transient absorption (fs-TA). Our findings on TEL21/M^+ are in good agreement with those obtained by Ma and Kwok[37] using broadband fs time-resolved fluorescence (fs-TRF); the latter publication also reported the first fs-TA study on GQs and examined their behavior in nanocavities. All these experiments were performed at room temperature with 266/267 nm excitation. Just one study, by Huppert et al., reported fluorescence of G-wires in low temperature glasses probed by TCSPC[38]; their results at room temperature are in qualitative agreement with ours on these systems.[39,40]

The time-resolved signals associated either with GQ fluorescence or their photoionization are weak. Therefore, their detection following excitation with laser pulses is quite delicate and requires specific protocols in order to avoid damaging the system during experiments.[20,21]

EXCITED STATE RELAXATION

Discussing the relaxation of electronic excited states in GQs requires some knowledge of those initially formed by photon absorption (Franck–Condon states). Several computational approaches showed that the electronic coupling among the ππ* transitions of nucleobases, which are responsible for the absorption spectrum of mononucleotides, induces delocalization of their Franck–Condon states over several guanines of the core.[39,41–47] The properties of the resulting exciton states depend on the relative position and orientation of the participating guanines, which may be located on the same strand or tetrad or on different ones. The topography of two such collective states, computed for $(G_3)_4/Na^+$ in the frame of the exciton theory, taking into account conformational static disorder, are shown in fig. 9 of reference Changenet-Barret et al.[39] Due to the existence of collective states, the GQ steady-state absorption (and CD) spectra are the envelope of a large number of electronic transitions, and differ from those of the corresponding stoichiometric mixtures of noninteracting mononucleotides. Figure 2A illustrates such a difference in the simplest case, comparing the absorption spectra of dGMP and self-associated GGG strands, $(G_3)_4/Na^+$.[22]

Once populated, the Franck–Condon states will evolve toward lower energies along various pathways[47] implying: (1) Changes in their topography, possibly leading to localization of excitons on single nucleobases. (2) Charge transfer (CT) between stacked nucleobases, requiring an orbital overlap and giving rise to an excited CT state, meaning that a certain fraction δ^+ of an atomic electric charge is transferred among them (upper panel in Figure 3). CT states may be formed between two guanines in the core, two peripheral nucleobases within loops or capping groups, or a peripheral nucleobase X and a guanine of an outer tetrad. According to quantum chemical calculations, the probability to populate a $G^+ \rightarrow X^-$ CT state is higher if X is an adenine than a thymine; moreover, CT formation is more favorable if the peripheral base is located at the 3′ position, in respect to the guanine, than in the 5′ position.[48]

Charge transfer formation is accompanied by a geometrical rearrangement of the involved chromophores and a readjustment of their close environment: the non-excited part of the nucleic acid, the nearby water molecules and the metal cations. In this way, the changes in the distribution of the atomic electronic charges are compensated, which further stabilizes the CT states, reducing their energy.[49] The larger the δ^+ value, the most important the necessary modifications leading to full stabilization of the system.

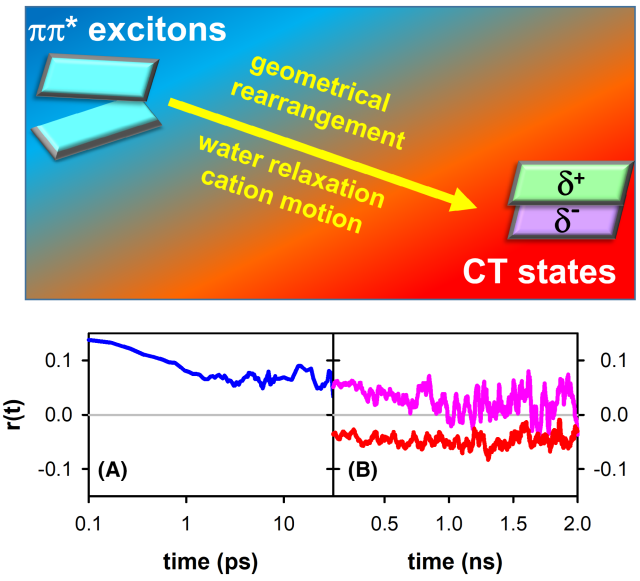

FIGURE 3 Upper panel: Schematic representation of the excited state relaxation leading from ππ* excitons to excited charge transfer (CT) states. Lower panel: time and wavelength dependence of the fluorescence anisotropy $r(t)$ probing these processes; (A) 330 nm; blue: OXY/K^+[36]; (B) 450 nm; pink: OXY/K^+[36] and red: $(TG_4T)_4/Na^+$.[64]

In GQs, excited state relaxation is seriously perturbed by structural constrains. First of all, the amino groups of the guanines in the core being engaged in hydrogen bonding, their out-of-plane movement, accompanying the decay of the ππ* states,[50,51] is slightly hampered. Moreover, the primary shell of water, playing an important role in the stabilization of CT states, is quite structured in the regions of the grooves and the loops; water molecules may be hydrogen bonded to the oxygen atoms of the phosphate and the sugar moieties, as well as to the nitrogen atoms of guanines, located at certain positions.[52] The characteristic rotation and residence times of water molecules are highly anisotropic and extend on the microsecond time,[53] that is, much longer than the lifetimes of singlet excited states. The consequence of the above constrains is that both exciton localization and stabilization of CT states are less efficient compared to other, less rigid, DNA systems. In particular, excited states with strong CT character, requiring important readjustment of their environment, are likely to decay before being fully stabilized, that is before reaching a minimum in the potential energy surface of the first excited state.

The above processes are expected to be highly anisotropic, depending on the location of the involved nucleobases. Their efficiency should decrease going from the capping groups to the loops and, finally, to the core. Likewise, when moving from outer to inner tetrads and upon replacing Na^+ by K^+ ions, whose mobility is lower.[53,54]

The inhomogeneity in the relaxation processes in GQs renders the currently performed analysis of time-resolved signals by multi-exponential quite problematic. Although such data treatment may be convenient for phenomenological comparisons, the resulting time constants do not necessarily correspond to precise transient species. This remark concerns not only the excited state dynamics,[21] but also the reaction dynamics of guanine radicals,[55] which will be discussed later.

FLUORESCENCE EMISSION

The fluorescence quantum yield of all GQs has been found to be higher (by at least a factor of 3) than those of the corresponding stoichiometric mixture of their constitutive mononucleotides. The fluorescence of mononucleotides in aqueous solution decays completely within a few ps.[56] Much longer lifetimes were found for all the studied GQs. Although their fluorescence starts decaying on the fs timescale, photons are still detected after 1 ns. However, most of the photons around the fluorescence maximum are emitted before 100 ps, as illustrated in Figure 4 for TEL21/Na^+.[45] G-wires are an exception to this rule, the majority of the photons being emitted after 100 ps.[40]

As explained in the previous section, GQ fluorescence stems from a large variety of excited states: ππ* localized on the guanines of the core or the peripheral bases, ππ* excitons (possibly exhibiting a weak CT character), CT states involving guanines and/or peripheral nucleobases, and having undergone partial or total solvent equilibration. Despite the important diversity of the emitting states, it is possible to identify the dominant type thanks to the fluorescence anisotropy $r(t)$.[21] The latter decreases very rapidly (in <300 fs) to a value close to 0.1, corresponding to in-plane depolarization of the fluorescence.[21] This is due to ultrafast energy transfer involving exciton states. Subsequently, as ππ* transitions are polarized within the aromatic plane of the nucleobases, they give rise to positive $r(t)$ values. In contrast, excited states with strong CT character are characterized by negative $r(t)$, arising from the presence of an important out-of-plane component.[57] Thus, the relaxation scheme shown in the upper panel of Figure 3 can be roughly monitored by probing $r(t)$, which generally decreases with the time and the emission wavelength (Figures A and B in the lower panel of Figure 3). For some GQs, but not all of them, $r(t)$ attains negative values after 0.1 ns (Figure 3B).

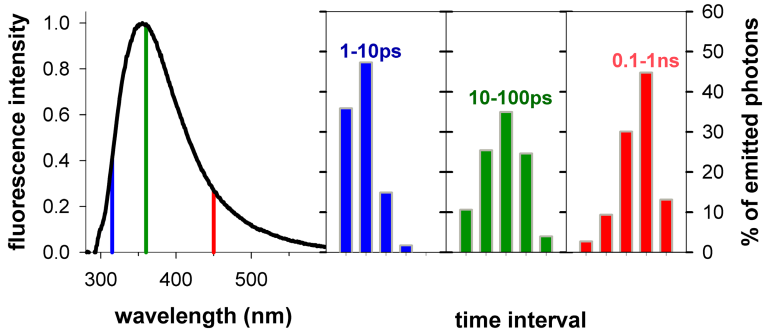

FIGURE 4 Fluorescence spectrum of TEL21/Na^+ obtained by exciting at 267 nm[45]; the vertical lines indicate the emission wavelengths (315, 360, and 450 nm) corresponding to the histograms on the right. Each histogram represents the percentage of photons emitted at a given wavelength over each one of the five time intervals: <1 ps, 1–10 ps, 10–100 ps, 0.1–1 ns, and ≥1 ns; they were derived from the joint fluorescence decays recorded by FU and TCSPC.

The fluorescence spectra of all the examined GQs stabilized by K^+ ions peak at 335 ± 5 nm, where $r(t)$ remains positive. This means that the dominant emission in these systems originates from ππ* states associated with the core, localized on single guanines or delocalized over a few of them, and possibly exhibiting some weak CT. A strong indication for emission from exciton states is provided by the spectral narrowing observed in the case G-wires/K^+, which contain exclusively guanines: the width (fwhm) of their fluorescence spectrum (5000 cm^{-1}) is much smaller than that dGMP (8600 cm^{-1}); see fig. 8 in reference Changenet-Barret et al.[58]

Replacement of K^+ ions by Na^+ ions, which are more mobile[59] and, hence, better contributing to the stabilization of the emitting states than K^+ ions, induces a shift of the fluorescence spectrum toward longer wavelengths.[37,40,58] Quantum chemistry calculations performed for TEL21/Na^+ identified the existence of a local minimum in the potential energy surface of the lower excited state.[45] At this point, the excitation is shared between two stacked guanines while a very small CT (δ = 0.06) takes place. The most striking change is the shortening of the stacking distance, from 3.6 Å in the ground state to 2.4 Å in the relaxed excited state. Due to this important structural distortion, the term "neutral excimer" was employed to designate this collective ππ* state. The stabilization of neutral excimers in TEL21/Na^+ shifts its fluorescence maximum to somewhat longer wavelengths, that is, at 360 nm (Figure 6A) instead of 340 nm for TEL21/K^+, and increases its fluorescence quantum yield by 30%.[45,60] A analogous trend was also observed for a longer human telomeric sequence.[27]

The nature of the metal cations in the solution may alter the folding topology of GQs. This is the case of the human telomeric sequence adopting hybrid or antiparallel topology in the presence of K^+ or Na^+ ions, respectively.[61,62] Topology determines the relative orientation of the guanine moieties, and hence, the electronic interactions among them. But the key factor for the observed fluorescence is rather the metal cation itself, whose size and mobility determines the ability of stacked guanines to come closer to each other. In this respect, it is worth noticing that a red shift in the fluorescence spectrum is also observed when going from OXY/K^+ to OXY/Na^+,[32] despite the fact that both systems exhibit the same antiparallel topology.[63] Similarly, the fluorescence maximum of $(G_3)_4$/Na^+ (340 nm)[22] is located at a longer wavelength compared to that of $(TG_3T)_4$/K^+ (330 nm),[64] both exhibiting a parallel topology. For all the examined GQs, with no regard to their topology, the dominant emission arises from ππ* states, as indicated from the fluorescence anisotropy determined close to the fluorescence maximum. Figure 5 shows that after ca. 3 ps, corresponding to the decay of the "monomer-like" emission, $r(t)$ acquires a similar value of

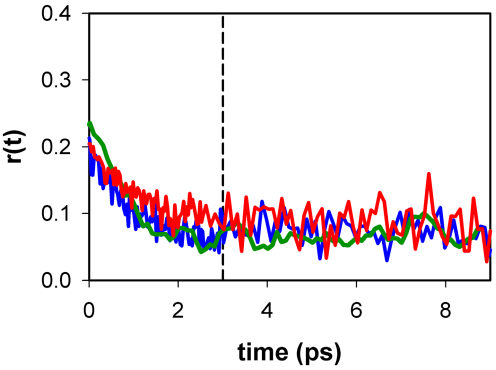

FIGURE 5 Fluorescence anisotropies recorded close to the fluorescence maximum for GQs composed of three tetrads and exhibiting different topologies. Green: parallel, $(TG_3T)_4/K^+$[64]; blue: hybrid, TEL21/K^+[60]; red: antiparallel, TEL21/Na^+.[45] The vertical dashed line indicates the time after which emission from localized "monomer-like" states is no more detected.

~0.09 ± 0.3 for systems with parallel, antiparallel or hybrid topology. According to the results reported by Ma and Kwok on TEL21/Na^+ and TEL21/K^+, this similarity extends over a much larger time domain; see fig. 3c in reference Ma et al.[37]

More favorable conditions for the excited state relaxation is encountered in $(TG_4T)_4/Na^+$, in which the mutual mobility of the four strands, facilitated by the lability of the Na^+ ions, may contribute to attain better orbital overlap between guanines and, hence, higher CT. As a matter of fact, its fluorescence spectrum exhibits an important shoulder at ~395 nm and its fluorescence anisotropy at the red part (Figure 3B) is the lowest detected among all the studied GQs. As excited states with strong CT character are weak emitters, its Φ_{fl} (3.0×10^{-4}) is also the lowest determined for any GQ.[65]

So far, we discussed the emission stemming from the core. But peripheral nucleobases also emit. As, in general, they have more degrees of freedom than the guanines of the core, they often follow a "monomer-like" ultrafast deactivation path and their contribution to the overall Φ_{fl} is small. However, two nucleobases located at the same loop or capping group may interact. Thus, "T–T" excimer emission stemming from the loops of OXY/K^+ and characterized by positive anisotropy was reported recently[36]; its contribution to the fluorescence spectrum is shown as green shaded area in Figure 6B. Furthermore, as demonstrated by quantum chemistry calculations, a peripheral nucleobase may interact with a guanine of an outer tetrad.[45,48] An experimental fingerprint of such "mixed" CT states is obtained by subtracting the fluorescence spectrum of the parallel GQ $(TG_5T_4)/K^+$ from that of (TG_3T_4)/K^+, for which the thymine/guanine ratio is higher. The difference between the two spectral shapes is shown as pink shaded are in Figure 6C. At the corresponding spectral

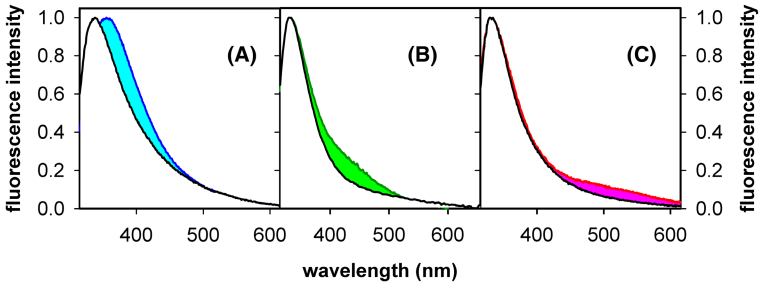

FIGURE 6 Emission from different types of excited states, appearing as colored areas between normalized steady-state fluorescence spectra of GQ pairs. (A) "G–G" neutral excimers (cyan); black: TEL21/K^+[60]; blue: TEL21/Na^+.[45] (B) "T–T" excimers in the diagonal loops (green); black: $(TG_4T)_4/K^+$[40]; green: OXY/K^+.[36] (C) $G^+ \rightarrow T^-$ charge transfer states (pink); black: $(TG_5T)_4/K^+$; red: $(TG_3T)_4/K^+$.[64] The peaks of the all spectra correspond to ππ* emission.

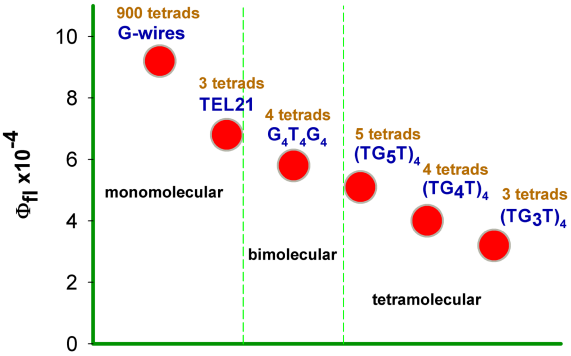

FIGURE 7 Fluorescence quantum yields determined for GQs stabilized by K^+ ions upon excitation at 267 nm. Data from references Balanikas et al., Hua et al., Changenet-Barret et al. and Hua et al.[36,40,60,64]

region, the fluorescence anisotropy gets negative values.[64] In contrast, as it can be observed in Figure 3B, no negative $r(t)$ was detected for OXY/K^+,[36] in which the motion of thymines in the loops is more restricted than that of the capping groups in $(TG_nT)/K^+$.

Figure 7 compares the Φ_{fl} values determined for a series of GQs stabilized by K^+ ions, whose fluorescence spectrum is dominated by emission from ππ* states: they range from 3.2×10^{-4} to 9.2×10^{-4} and are all higher than those reported for duplexes.[21] We remark that Φ_{fl} decreases when the molecularity of the GQ increases. This is concomitant with an acceleration of the fluorescence decays. Thus, the photons emitted after 0.1 ns around the fluorescence maximum correspond to 45% of the total for G-wires/K^+,[40] 18.2% for OXY/K^+[36] and only 7.5% for $(TG_4T)_4/K^+$.[40]

Although less data obtained under comparable conditions are available for GQs stabilized by Na^+ ions, a similar trend is observed: the Φ_{fl} of the tetramolecular $(TG_4T)_4/Na^+$ (3.0×10^{-4})[65] is much lower compared to those of the monomolecular TEL21/Na^+ (8.7×10^{-4})[45] and G-wires/Na^+ (9.2×10^{-4}).[40]

The Φ_{fl} variation with the GQ molecularity is explained by the fact that conformational motions at the end of strands are more important than in their inner parts, in particular when they contain dangling groups. Such motions contribute to the breaking down the coherence of the collective states and reduce Φ_{fl}. The same factor could also explain, at least partially, why the Φ_{fl} of $(TG_nT)_4/K^+$ decreases upon decreasing the number of guanines per strand[64]; an additional factor is that an increasing part of the excitations evolves toward $G^+ \rightarrow T^-$ CT states (Figure 6C), which exhibit very low oscillator strength[48] and, hence, are weakly emissive. Alternatively, conformational motions can be reduced in confined media. Thus, the Φ_{fl} reported for TEL21/Na^+ confined in reversed AOT micelles is 20% higher, and its lifetime longer compared to the same system in aqueous solution.[37] We also note that the difference in Φ_{fl} between monomolecular GQs with three tetrads and the very long G-wires is relatively small. The reason could be that there is a saturation effect or that the G-wires, are possibly composed of multiple interconnected smaller GQ structures.[66] It would be worthy to examine how the Φ_{fl} of monomolecular GQs with well-defined structures evolves upon increasing the number of tetrads up to 5 or 6.

The interaction among the guanines of the core and the loop nucleobases could be responsible for a peculiar fluorescence component appearing at the blue part of the spectrum and decaying on the ns timescale. Although such high-energy long-lived fluorescence, correlated with collective excited states, is ubiquitous in duplexes,[67] it was detected just for one four-stranded structure, OXY/K^+.[36] Further studies are needed to elucidate the geometrical and electronic features of these emitting states.

Much more elusive than the above high-energy ns emission is the origin of another band, also decaying on the ns timescale, but peaking around 385 nm. It was observed for a series of structures whose main representative is $(G_3TG_3TG_3TG_3T)_4/K^+$.[68,69] This band was initially

attributed to excimers resulting from the 5/6 overlap of guanines in the interface between two stacked GQ blocks.[68] Later studies on stacked GQs with various interface patterns showed the 5/6 overlap is not a necessary condition for the appearance of this emission, which depends also on the topology of each individual GQ[34]; the latter conclusions were drawn from steady-state fluorescence measurements, without determination of quantum yields, and the role of the peripheral bases was neglected in the discussion. The effect of the peripheral nucleobases was carefully examined by another group, challenging the interpretation of stacked GQs[33,69]; a strong argument was the fact that the excimer emission is not affected by the salt concentration, expected to favor GQ stacking. However, the electronic coupling between the thymines in the loops and the core was precluded as possible origin of the excimer emission, since it persists even in the presence of abasic loops.[69] Given that the intensity of this band is at least twice as high as that of the monomeric GQs[69] reported here, a comprehensive study, considering the fate of electronic excitations in the entire system, accompanied by theoretical calculations, is worthy to be undertaken. The same remark is also valid for the highly fluorescent left-handed GQs ($\Phi_{fl} \sim 2\times10^{-3}$) reported by Zuffo et al.[27] However, prior to any complex investigation on these stems, it is important to record their emission under the same conditions as those used for the results reported here, that is, in phosphate buffer prepared with high purity (>99.99%) salts.

CHARGE CARRIER GENERATION

Closely related to the excited state relaxation, GQ photoionization provoked by direct absorption of low-energy photons generates two types of different charge carriers, hydrated electrons and guanine radical cations, in equal concentrations.[20] These transient species have been identified and quantified by ns transient absorption spectroscopy.[23,48,55,70–73] Although the photoionization of other DNA structures in aqueous solutions was initially studied at high energies, exciting at wavelengths shorter than 200 nm,[74–76] that of GQs was investigated only with excitation at 266 nm. The latter wavelength corresponds to an energy (4.7 eV) significantly lower than the vertical ionization potentials (>6.6 eV) determined for nucleic acids,[77–79] even when they are arranged in four-stranded structures.[72]

In contrast to high-energy photoionization, where the electron is ejected directly upon excitation, prior to any geometrical arrangement, low-energy photoionization takes place via a complex mechanism.[24] The latter likely involves formation of excited CT states, charge separation, trapping of the electron hole by the core, and electron ejection from the nucleobase bearing the negative charge (Figure 8).

A first key factor underlying the above photoionization scheme is the oxidation potential of the nucleobases. That of guanine is the lowest among the DNA bases, and it is farther decreased upon stacking.[80,81] GG and GGG stacks are known to act as traps for hole migration.[82–85] Deviations from an ideal stacking associated with a strongly anisotropic environment are expected to induce variations of the oxidation potential. In this way, a guanine of an outer tetrad may behave as the "peripheral" nucleobase in Figure 8. A second key factor is that the vertical ionization potential of a negatively charged nucleobase is quite low;[86] consequently, the latter nucleobase can easily eject an electron.

An important finding is that the photoionization quantum yields determined for GQs at 266 nm (Figure 9) exceed by one order of magnitude their Φ_{fl}. Moreover, they are all higher than those found for duplexes, while no photoionization was observed for mononucleotides ($\Phi_i < 3\times10^{-4}$), neither for most of the examined single strands.[20]

Alike fluorescence, the propensity of GQs to undergo low-energy photoionization depends on certain structural parameters. But although the number of constitutive strands and the number of tetrads affect Φ_{fl} (Figure 7), they do not seem to play an important role on Φ_i (Figure 10). Neither a topology effect was detected. The studies performed so far reveled two essential elements: the metal cations in the central cavity and the peripheral nucleobases.

Figure 10 shows that all the Φ_i values determined for GQs in the presence of K^+ ions are higher than those found for Na^+ solutions. This is attributed to the effect of the

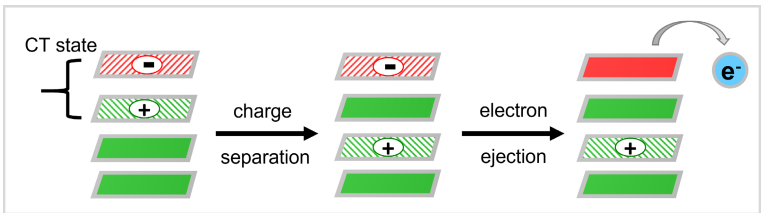

FIGURE 8 Schematic illustration of the GQ photoionization mechanism by low-energy photons. For simplicity, only one guanine strand (green) and one peripheral nucleobase (red) are shown. Shaded areas denote electrically charged nucleobases.

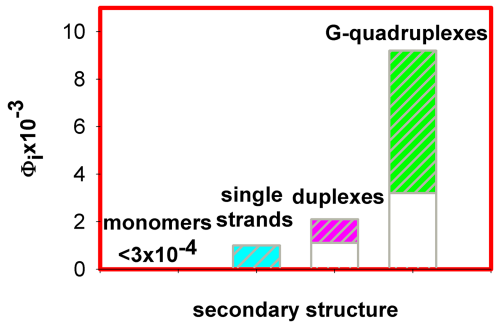

FIGURE 9 Effect of the secondary structure on the DNA photoionization quantum yields determined following excitation at 266 nm; the values corresponding to GQs, duplexes, and single strands are located, respectively, within the areas shaded in green, pink, and cyan. Data from references Balanikas et al. and Balanikas et al.[20,48]

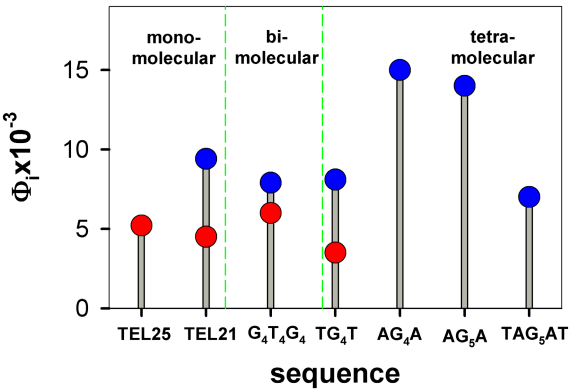

FIGURE 10 Photoionization quantum yields determined for GQs in the presence of K^+ (blue) or Na^+ (red) ions following excitation at 266 nm. Data from references Balanikas et al. and Balanikas et al.[20,48]

central ions on the step of charge separation (Figure 8). As mentioned previously Na^+ ions favor the stabilization of the excited states involving stacked guanines. This implies that the two guanines come closer together, decreasing the probability for the electron hole to migrate to the next, non-excited, guanine. As a result, charge recombination, leading to ground state is favored, while charge separation becomes less probable.

The role of the peripheral bases on the Φ_i was evidenced by study of tetramolecular GQs, formed by both symmetric 5′-XG_4X-3′ and asymmetric 5′-XG_4-3′/5′-G_4X-3′ strands, with X = adenine or thymine.[48] For all three types of systems, those containing adenines have a higher Φ_i compared to their thymine counterparts (Figure 11). Moreover, the Φ_i found for GQs with peripheral nucleobases located at the 3′ ends are higher than their analogs with peripheral nucleobases on the 5′ ends. These trends are in line with the computed probability to populate a $G^+ \rightarrow X^-$ CT state

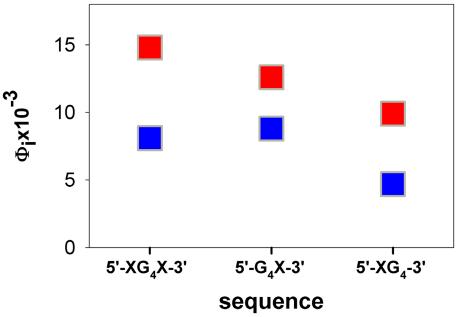

FIGURE 11 Effect of the capping groups on the photoionization quantum yields determined for tetramolecular GQs in the presence of K^+ ions following excitation at 266 nm; X = adenine: red; X = thymine: blue. Data from reference Balanikas et al.[48]

during the excited state relaxation,[48] which is reduced if a second nucleobase is present in the capping groups. In such a case, an additional pathway opens up, leading to CT formation between two peripheral bases. A typical example is $(TAG_4AT)_4/K^+$, whose Φ_i is half that of $(AG_4A)_4/K^+$ (Figure 10).

Regarding the dynamics of the charge carriers, hydrated electrons survive in neat water for several ms.[87] In most of the time-resolved experiments reported here, their lifetime was artificially shortened to 500 ns, so that to avoid their interference in the study of the guanine radicals on the μs and ms timescales. As $H_2PO_4^-$ ions are known to be efficient scavengers of hydrated electrons,[87] their lifetime can be tuned by adjusting the concentration of the phosphate buffer.

$(G^+)^\bullet$ radicals in neutral pH are unstable and tend to eject a proton to water, thus losing their electric charge. They also may disappear via other chemical reactions.[23,88,89] Their lifetime in genomic DNA is 330 ns.[20] But, because of the GQ anisotropic nature, including that of the water network, the decay of the $(G^+)^\bullet$ population follows a more complex pattern, being composed roughly of two parts[90]: a fast one, which can be approximated by time constants of 150–200 ns, and a slower one, completed within a few tens of μs. Theoretical calculations, performed for TEL21/M^+ containing an electron hole, showed that the deprotonation conditions are more favorable when $(G^+)^\bullet$ is located in an outer tetrad, and, thus, more exposed to water.[91] Accordingly, the fast deprotonation step could be correlated with outer tetrads while the slow one with the inner ones. Experimentally, it was found that the percentage of the initially generated population of $(G^+)^\bullet$ still surviving at 2 μs ranges from 25% to 60%.[90] However, the existing studies do not allow establishing a rational concerning the factors that underly these numbers because of the specific solvation patterns associated with each GQ structure and possible competition among various reactions.

SUMMARY AND OUTLOOK

The studies on the primary processes triggered in GQs by direct absorption of UV radiation had not been undertaken in connection with future applications. Yet, their understanding helps clarifying some points and drawing a few rules toward this direction.

Fluorescence emission and charge carrier generation strongly depend on the pathways followed during the excited state relaxation, which is greatly affected by structural parameters. In both cases, the population of CT states plays a key role, albeit not in the same way. For example, the formation of CT states between a guanine of the core and a peripheral nucleobase is beneficial for the generation of charge carriers, while it is detrimental to the fluorescence emission. Consequently, the relaxation pathways leading to such states may be controlled by adjusting the appropriate structural elements, so that to enhance or suppress their population in function of the type of signal to be optimized, in view of a desired application. A few guidelines, deduced from the discussion in the previous sections, are summarized on Table 2.

Regarding the optimization of the fluorescence signal, it is preferable to privilege emission of ππ* states stemming from the core, which corresponds to the maximum of all the fluorescence spectra. Its intensity increases upon reducing the molecularity and increasing the number of tetrads. In contrast, it is important to eliminate the pathways leading to weakly emissive CT states or localized ππ* states of peripheral nucleobases, which result in a broadening of the spectrum and reduce the peak intensity. This can be achieved by avoiding the presence of capping groups and limiting the number of nucleobases in the loops.

As far as the generation of charge carriers is concerned, it appears clearly that it is favored by K^+ ions, as well as by the presence of adenines at the 3′ position in respect to the guanines of the core. These peripheral nucleobases need to have sufficient degrees of freedom to form an excited state $G^+ \rightarrow X^-$ with a strong CT character.

All Φ_{fl} and Φ_i values determined for GQs are significantly higher than those of duplexes. These values have been found for excitation at 266/267 nm because of the availability of the laser sources used in the time-resolved experiments. Yet, the collective nature of the GQ Franck–Condon states is more pronounced in the 290–300 nm spectral domain (Figure 2A). Steady-state experiments, already tempted in the case of fluorescence emission,[22,29] could further assess whether there is an appreciable gain in signal intensity, compensating the weaker absorption cross section in the red edge of the spectrum. Charge generation via low-energy photoionization was discovered just 6 years ago and ever since only fundamental studies, aiming at the understanding of this unexpected effect, have been reported. At this stage, wavelength-dependent photoelectrochemical measurements could be very useful, before envisioning the development of devices based on this principle. Such a perspective seems particularly interesting because the photoionization quantum yields, $(3.2–9.2)\times10^{-3}$, are higher by one order of magnitude compared to those of fluorescence, $(3.0–9.5)\times10^{-4}$.

Photoionization-based devices are likely to be more efficient for the discrimination among different secondary structures (Figure 9). While the fluorescence assays presented in reference Zuffo et al.[27] are more appealing for the rapid screening of a very large number of sequences, the photoionization method could be interesting for the detection of GQ forming sequences of nucleic acids related with a given pathology. Both methods are, in principle, suitable for detecting metal ions but none of them exhibits enough precision for discriminating among different topologies. Regarding the recognition of target molecules that bind to GQs without altering their structure, the use of the intrinsic fluorescence is irrelevant, because the presence of these species should hardly affect the excited state relaxation. But we can speculate that photoionization-based devices could allow the detection of such analytes if they have an appropriate redox potential so that to behave as the peripheral base in Figure 8.

TABLE 2 Guidelines for optimization of the signals generated upon GQ excitation at 266/267 nm, derived from the study of primary processes.

Fluorescence emission	Charge carrier generation
Reduce number of strands	Privilege K^+ over Na^+
Increase number of tetrads	Peripheral bases: • Privilege 3′ over 5′ position • Privilege adenines over thymines
Avoid capping groups	
Reduce number of nucleobases in loops	

ACKNOWLEDGMENTS

I am grateful to my colleagues and collaborators: Drs E. Balanikas, A. Banyasz, P. Changenet, T. Gustavsson, R. Improta, and L. Martinez-Fernandez, with whom I worked, over the years, on the study of guanine-quadruplexes.

ORCID

Dimitra Markovitsi https://orcid.org/0000-0002-2726-305X

REFERENCES

1. Largy E, Gabelica V, Mergny J. Basics of G-Quadruplex structures. 2020. Accessed May 28, 2023. https://ericlarg4.github.io/Distill_section/docs/guideline.html

2. Wang E, Thombre R, Shah Y, Latanich R, Wang JO. G-quadruplexes as pathogenic drivers in neurodegenerative disorders. *Nucleic Acids Res*. 2021;49:4816-4830.
3. Tateishi-Karimata H, Sugimoto N. Roles of non-canonical structures of nucleic acids in cancer and neurodegenerative diseases. *Nucleic Acids Res*. 2021;49:7839-7855.
4. Blackburn EH, Epel ES, Lin J. Human telomere biology: a contributory and interactive factor in aging, disease risks, and protection. *Science*. 2015;350:1193-1198.
5. Endoh T, Takahashi S, Sugimoto N. Endogenous G-quadruplex-forming RNAs inhibit the activity of SARS-CoV-2 RNA polymerase. *Chem Commun (Camb)*. 2023;59:872-875.
6. Goswami P, Bartas M, Lexa M, et al. SARS-CoV-2 hot-spot mutations are significantly enriched within inverted repeats and CpG Island loci. *Brief Bioinform*. 2021;22:1338-1345.
7. Yu ZT, Spiegel J, Melidis L, et al. Chem-map profiles drug binding to chromatin in cells. *Nat Biotechnol*. 2023. doi:10.1038/s41587-022-01636-0
8. Toro PM, Saldias M, Valenzuela-Barra G. Metal-organic compounds as anticancer agents: versatile building blocks for selective action on G-quadruplexes. *Curr Med Chem*. 2023;30:573-600.
9. Moraca F, Marzano S, D'Amico F, et al. Ligand-based drug repurposing strategy identified SARS-CoV-2 RNA G-quadruplex binders. *Chem Commun (Camb)*. 2022;58:11913-11916.
10. Mergny JL, Sen D. DNA quadruple helices in nanotechnology. *Chem Rev*. 2019;119:6290-6325.
11. Yang HL, Zhou Y, Liu JW. G-quadruplex DNA for construction of biosensors. *TrAC Trends Anal Chem*. 2020;132:116060.
12. Liu JX, Yan L, He SL, Hu JQ. Engineering DNA quadruplexes in DNA nanostructures for biosensor construction. *Nano Res*. 2022;15:3504-3513.
13. Yu XH, Zhang SQ, Guo WQ, et al. Recent advances on functional nucleic-acid biosensors. *Sensors*. 2021;21:7109.
14. Xu JQ, Jiang RD, He HL, Ma CB, Tang ZW. Recent advances on G-quadruplex for biosensing, bioimaging and cancer therapy. *Trends Anal Chem*. 2021;139:116257.
15. Smith AF, Zhao B, You MX, Jimenez JM. Microfluidic DNA-based potassium nanosensors for improved dialysis treatment. *Biomed Eng Online*. 2019;18:73.
16. Xi H, Juhas M, Zhang Y. G-quadruplex based biosensor: a potential tool for SARS-CoV-2 detection. *Biosens Bioelectron*. 2020;167:112494.
17. Hudecova I, Smith CG, Hansel-Hertsch R, et al. Characteristics, origin, and potential for cancer diagnostics of ultrashort plasma cell-free DNA. *Genome Res*. 2022;32:215-227.
18. Wang Y, Li J, Qiao P, et al. Screening and application of a new aptamer for the rapid detection of Sudan dye III. *Eur J Lipid Sci Technol*. 2018;120(6):1700112.
19. Zhu NX, Liu XN, Peng KM, et al. A novel aptamer-imprinted polymer-based electrochemical biosensor for the detection of lead in aquatic products. *Molecules*. 2023;28:196.
20. Balanikas E, Banyasz A, Douki T, Baldacchino G, Markovitsi D. Guanine radicals induced in DNA by low-energy photoionization. *Acc Chem Res*. 2020;53:1511-1519.
21. Gustavsson T, Markovitsi D. Fundamentals of the intrinsic DNA fluorescence. *Acc Chem Res*. 2021;54:1226-1235.
22. Markovitsi D, Gustavsson T, Sharonov A. Cooperative effects in the photophysical properties of self-associated triguanosine diphosphates. *Photochem Photobiol*. 2004;79:526-530.
23. Banyasz A, Martinez-Fernandez L, Balty C, et al. Absorption of low-energy UV radiation by human telomere G-quadruplexes generates long-lived guanine radical cations. *J Am Chem Soc*. 2017;139:10561-10568.
24. Balanikas E, Markovitsi D. DNA photoionization: from high to low energies. In: Improta R, Douki T, eds. *DNA Photodamage: From Light Absorption to Cellular Responses and Skin Cancer*. RSC; 2021:37-54.
25. Martinez-Fernandez L, Santoro F, Improta R. Nucleic acids as a playground for the computational study of the photophysics and photochemistry of multichromophore assemblies. *Acc Chem Res*. 2022;55:2077-2087.
26. Xiang X, Li Y, Ling L, Bao Y, Su Y, Guo X. Label-free and dye-free detection of target DNA based on intrinsic fluorescence of the (3+1) interlocked bimolecular G-quadruplexes. *Sensors Actuators B Chem*. 2019;290:68-72.
27. Zuffo M, Gandolfini A, Heddi B, Granzhan A. Harnessing intrinsic fluorescence for typing of secondary structures of DNA. *Nucleic Acids Res*. 2020;48:e61.
28. Lu C, Lopez A, Zheng JK, Liu JW. Using the intrinsic fluorescence of DNA to characterize aptamer binding. *Molecules*. 2022;27:7809.
29. Lopez A, Liu J. Probing metal-dependent G-quadruplexes using the intrinsic fluorescence of DNA. *Chem Commun (Camb)*. 2022;58:10225-10228.
30. Assi S, Abbas I, Arafat B, Evans K, Al-Jumeily D. Authentication of Covid-19 vaccines using synchronous fluorescence spectroscopy. *J Fluoresc*. 2023;33:1165-1174.
31. Mendez MA, Szalai VA. Fluorescence of unmodified oligonucleotides: a tool to probe G-quadruplex DNA structure. *Biopolymers*. 2009;91:841-850.
32. Dao NT, Haselsberger R, Michel-Beyerle ME, Phan AT. Following G-quadruplex formation by its intrinsic fluorescence. *FEBS Lett*. 2011;585:3969-3977.
33. Kwok CK, Sherlock ME, Bevilacqua PC. Effect of loop sequence and loop length on the intrinsic fluorescence of G-quadruplexes. *Biochemistry*. 2013;52:3019-3021.
34. Gao S, Cao Y, Yan Y, Xiang X, Guo X. Correlations between fluorescence emission and base stacks of nucleic acid G-quadruplexes. *RSC Adv*. 2016;6:94531-94538.
35. Feng H, Kwok CK. Spectroscopic analysis reveals the effect of hairpin loop formation on G-quadruplex structures. *RSC Chem Biol*. 2022;3:431-435.
36. Balanikas E, Gustavsson T, Markovitsi D. Fluorescence of bimolecular guanine quadruplexes: from femtoseconds to nanoseconds. *J Phys Chem B*. 2023;127:172-179.
37. Ma CS, Chan RC-T, Chan CT-L, Wong AK-W, Kwok W-M. Real-time monitoring excitation dynamics of human telomeric guanine quadruplexes: effect of folding topology, metal cation, and confinement by nanocavity water pool. *J Phys Chem Lett*. 2019;10:7577-7585.
38. Gepshtein R, Huppert D, Lubitz I, Amdursky N, Kotlyar AB. Radiationless transitions of G4 wires and dGMP. *J Phys Chem C*. 2008;112:12249-12258.
39. Changenet-Barret P, Emanuele E, Gustavsson T, et al. Optical properties of guanine nanowires: experimental and theoretical study. *J Phys Chem C*. 2010;114:14339-14346.
40. Hua Y, Changenet-Barret P, Improta R, et al. Cation effect on the electronic excited states of guanine nanostructures studied

by time-resolved fluorescence spectroscopy. *J Phys Chem Lett*. 2012;116:14682-14689.
41. Randazzo A, Spada GP, da Silva MW. Circular dichroism of quadruplex structures. *Top Curr Chem*. 2013;330:67-86.
42. Improta R. Quantum mechanical calculations unveil the structure and properties of the absorbing and emitting excited electronic states of guanine quadruplex. *Chem Eur J*. 2014;20:8106-8115.
43. Gattuso H, Spinello A, Terenzi A, Assfeld X, Barone G, Monari A. Circular dichroism of DNA G-quadruplexes: combining modeling and spectroscopy to unravel complex structures. *J Phys Chem B*. 2016;120:3113-3121.
44. Loco D, Jurinovich S, Di Bari L, Mennucci B. A fast but accurate excitonic simulation of the electronic circular dichroism of nucleic acids: how can it be achieved? *Physiol Chem Phys*. 2016;18:866-877.
45. Martinez-Fernandez L, Changenet P, Banyasz A, Gustavsson T, Markovitsi D, Improta R. A comprehensive study of guanine excited state relaxation and photoreactivity in G-quadruplexes. *J Phys Chem Lett*. 2019;10:6873-6877.
46. Avagliano D, Tkaczyk S, Sanchez-Murcia PA, Gonzalez L. Enhanced rigidity changes ultraviolet absorption: effect of a merocyanine binder on G-quadruplex photophysics. *J Phys Chem Lett*. 2020;11:10212-10218.
47. Martinez-Fernandez L, Esposito L, Improta R. Studying the excited electronic states of guanine rich DNA quadruplexes by quantum mechanical methods: main achievements and perspectives. *Photochem Photobiol Sci*. 2020;19:436-444.
48. Balanikas E, Martinez-Fernadez L, Improta R, Podbevsek P, Baldacchino G, Markovitsi D. The structural duality of nucleobases in guanine quadruplexes controls their low-energy photoionization. *J Phys Chem Lett*. 2021;12:8309-8313.
49. Nandi N, Bhattacharyya K, Bagchi B. Dielectric relaxation and solvation dynamics of water in complex chemical and biological systems. *Chem Rev*. 2000;100:2013-2046.
50. Improta R, Santoro F, Blancafort L. Quantum mechanical studies on the photophysics and the photochemistry of nucleic acids and nucleobases. *Chem Rev*. 2016;116:3540-3593.
51. Karunakaran V, Kleinermanns K, Improta R, Kovalenko SA. Photoinduced dynamics of guanosine monophosphate in water from broad-band transient absorption spectroscopy and quantum-chemical calculations. *J Am Chem Soc*. 2009;131:5839-5850.
52. Li K, Yatsunyk L, Neidle S. Water spines and networks in G-quadruplex structures. *Nucleic Acids Res*. 2021;49:519-528.
53. Snoussi K, Halle B. Internal sodium ions and water molecules in guanine quadruplexes: magnetic relaxation dispersion studies of d(G(3)T(4)G(3)) (2) and d(G(4)T(4)G(4)) (2). *Biochemistry*. 2008;47:12219-12229.
54. Balasubramanian S, Senapati S. Dynamics and barrier of movements of sodium and potassium ions across the *Oxytricha nova* G-quadruplex Core. *J Phys Chem B*. 2020;124:11055-11066.
55. Balanikas E, Banyasz A, Baldacchino G, Markovitsi D. Populations and dynamics of guanine radicals in DNA strands: direct versus indirect generation. *Molecules*. 2019;24:2347.
56. Gustavsson T, Improta R, Markovitsi D. DNA/RNA: building blocks of life under UV irradiation. *J Phys Chem Lett*. 2010;1:2025-2030.
57. Spata VA, Matsika S. Photophysical deactivation pathways in adenine oligonucleotides. *Phys Chem Chem Phys*. 2015;17:31073-31083.
58. Changenet-Barret P, Hua Y, Markovitsi D. Electronic excitations in guanine quadruplexes. *Top Curr Chem*. 2015;356:183-202.
59. Akhshi P, Mosey NJ, Wu G. Free-energy landscapes of ion movement through a G-quadruplex DNA channel. *Angew Chem Int Ed Engl*. 2012;51:2850-2854.
60. Changenet-Barret P, Hua Y, Gustavsson T, Markovitsi D. Electronic excitations in G-quadruplexes formed by the human telomeric sequence: a time-resolved fluorescence study. *Photochem Photobiol*. 2015;91:759-765.
61. Wang Y, Patel DJ. Solution structure of the human telomeric repeat $d[AG_3(T_2AG_3)_3]$ G-tetratraplex. *Structure*. 1993;1:263-282.
62. Phan AT, Luu KN, Patel DJ. Different loop arrangements of intramolecular human telomeric (3+1) G-quadruplexes in K^+ solution. *Nucleic Acids Res*. 2006;34:5715-5719.
63. Schultze P, Hud NV, Smith FW, Feigon J. The effect of sodium, potassium and ammonium ions on the conformation of the dimeric quadruplex formed by the *Oxytricha nova* telomere repeat oligonucleotide d(G(4)T(4)G(4)). *Nucleic Acids Res*. 1999;27:3018-3028.
64. Hua Y, Changenet-Barret P, Gustavsson T, Markovitsi D. The effect of size on the optical properties of guanine nanostructures: a femtosecond to nanosecond study. *Phys Chem Chem Phys*. 2013;15:7396-7402.
65. Miannay FA, Banyasz A, Gustavsson T, Markovitsi D. Excited states and energy transfer in G-quadruplexes. *J Phys Chem C*. 2009;113:11760-11765.
66. Chaires BJ, Graves D, eds. Quadruplex nucleic acids. *Topics in Current Chemistry*, Vol. 330. Springer; 2013.
67. Gustavsson T, Markovitsi D. The ubiquity of high-energy nanosecond fluorescence in DNA duplexes. *J Phys Chem Lett*. 2023;14:2141-2147.
68. Dao NT, Haselsberger R, Michel-Beyerle ME, Phan AT. Excimer formation by stacking G-quadruplex blocks. *ChemPhysChem*. 2013;14:2667-2671.
69. Sherlock ME, Rumble CA, Kwok CK, Breffke J, Maroncelli M, Bevilacqua PC. Steady-state and time-resolved studies into the origin of the intrinsic fluorescence of G-quadruplexes. *J Phys Chem B*. 2016;120:5146-5158.
70. Banyasz A, Balanikas E, Martinez-Fernandez L, et al. Radicals generated in tetramolecular guanine quadruplexes by photoionization: spectral and dynamical features. *J Phys Chem B*. 2019;123:4950-4957.
71. Balanikas E, Banyasz A, Baldacchino G, Markovitsi D. Guanine radicals generated in telomeric G-quadruplexes by direct absorption of low-energy UV photons: effect of potassium ions. *Molecules*. 2020;25:2094.
72. Behmand B, Balanikas E, Martinez-Fernandez L, et al. Potassium ions enhance guanine radical generation upon absorption of low-energy photons by G-quadruplexes and modify their reactivity. *J Phys Chem Lett*. 2020;11:1305-1309.
73. Balanikas E, Martinez-Fernandez L, Baldacchino G, Markovitsi D. Electron holes in G-quadruplexes: the role of adenine ending groups. *Int J Mol Sci*. 2021;22:13436.
74. Candeias LP, Steenken S. Ionization of purine nucleosides and nucleotides and their components by 193-nm laser photolysis in aqueous solution: model studies for oxidative damage of DNA. *J Am Chem Soc*. 1992;114:699-704.
75. Candeias LP, Oneill P, Jones GDD, Steenken S. Ionization of polynucleotides and DNA in aqueous solution by 193 nm

pulsed laser light—identification of base-derived radicals. *Int J Radiat Biol*. 1992;61:15-20.
76. Melvin T, Plumb MA, Botchway SW, Oneill P, Parker AW. 193 nm light induces single-strand breakage of DNA predominantly at guanine. *Photochem Photobiol*. 1995;61:584-591.
77. Slavicek P, Winter B, Faubel M, Bradforth SE, Jungwirth P. Ionization energies of aqueous nucleic acids: photoelectron spectroscopy of pyrimidine nucleosides and ab initio calculations. *J Am Chem Soc*. 2009;131:6460-6467.
78. Schroeder CA, Pluharova E, Seidel R, et al. Oxidation half-reaction of aqueous nucleosides and nucleotides via photoelectron spectroscopy augmented by ab initio calculations. *J Am Chem Soc*. 2015;137:201-209.
79. Pluharova E, Slavicek P, Jungwirth P. Modeling photoionization of aqueous DNA and its components. *Acc Chem Res*. 2015;48:1209-1217.
80. Meggers E, Michel-Beyerle ME, Giese B. Sequence dependent long range hole transport in DNA. *J Am Chem Soc*. 1998;120:12950-12955.
81. Saito I, Nakamura T, Nakatani K, Yoshioka Y, Yamaguchi K, Sugiyama H. Mapping of the hot spots for DNA damage by one-electron oxidation: efficacy of GG doublets and GGG triplets as a trap in long-range hole migration. *J Am Chem Soc*. 1998;120:12686-12687.
82. Giese B, Amaudrut J, Köhler A-K, Spormann M, Wessely S. Direct observation of hole transfer through DNA by hopping between adenine bases and by tunneling. *Nature*. 2001;412:318-320.
83. Barnett RN, Cleveland CL, Joy A, Landman U, Schuster GB. Charge migration in DNA: ion-gated transport. *Science*. 2001;294:567-571.
84. Takada T, Kawai K, Fujitsuka M, Majima T. Direct observation of hole transfer through double-helical DNA over 100 Å. *Proc Natl Acad Sci USA*. 2004;101:14002-14006.
85. Renaud N, Harris MA, Singh APN, et al. Deep-hole transfer leads to ultrafast charge migration in DNA hairpins. *Nat Chem*. 2016;8:1015-1021.
86. Schiedt J, Weinkauf R, Neumark DM, Schlag EW. Anion spectroscopy of uracil, thymine and the amino-oxo and amino-hydroxy tautomers of cytosine and their water clusters. *Chem Phys*. 1998;239:511-524.
87. Buxton GV, Greenstock CL, Helman WP, Ross AB. Critical review of rate constants for reactions of hydrated electrons, hydrogen atoms and hydroxyl radicals ($^{\cdot}OH/^{\cdot}O^{-}$) in aqueous solution. *J Phys Chem Ref Data*. 1988;17:513-886.
88. Cadet J, Wagner JR, Angelov D. Biphotonic ionization of DNA: from model studies to cell. *Photochem Photobiol*. 2019;95:59-72.
89. Fleming AM, Burrows CJ. G-quadruplex folds of the human telomere sequence alter the site reactivity and reaction pathway of guanine oxidation compared to duplex DNA. *Chem Res Toxicol*. 2013;26:593-607.
90. Balanikas E, Banyasz A, Baldacchino G, Markovitsi D. Deprotonation dynamics of guanine radical cations. *Photochem Photobiol*. 2022;98:523-531.
91. Asha H, Green JA, Esposito L, Santoro F, Improta R. Computing the electronic circular dichroism spectrum of DNA quadruple helices of different topology: a critical test for a generalized excitonic model based on a fragment diabatization. *Chirality*. 2023;35:298-310.
92. Behmand B, Balanikas E, Martinez-Fernandez L, et al. Correction to "potassium ions enhance guanine radical generation upon absorption of low-energy photons by G-quadruplexes and modify their reactivity". *J Phys Chem Lett*. 2020;11:2742.

AUTHOR BIOGRAPHY

Dimitra Markovitsi, after graduating from the National Technical University of Athens, received a PhD/Habilitation from the "Louis Pasteur" University (Strasbourg) in 1983. She joined the French National Center for Scientific Research (CNRS), where she is currently Emeritus Research Director. She has expertise in photophysics and photochemistry, with emphasis on time-resolved spectroscopy and interchromophore interactions. For more than two decades, she has been focusing her efforts on the study of UV-induced processes in DNA, from photon absorption to excited state relaxation and reaction dynamics.

How to cite this article: Markovitsi D. Processes triggered in guanine quadruplexes by direct absorption of UV radiation: From fundamental studies toward optoelectronic biosensors. *Photochem Photobiol*. 2023;00:1-13. doi:10.1111/php.13826